https://doi.org/10.5194/egusphere-2026-1225
Preprint. Discussion started: 9 March 2026

Intraseasonal prediction of monthly storminess in the North Sea with the ACE2 atmospheric emulator and Random Forests

Proshonni Aziz[1], Birgit Hünicke[1], and Eduardo Zorita[1]

[1]Institute of Coastal Systems – Analysis and Modeling, Helmholtz-Zentrum Hereon, Geesthacht, Germany

Correspondence: Proshonni Aziz (proshonni.aziz@hereon.de)

Abstract. This research explores the predictability of seasonal storminess in the North Sea using machine learning methods and the weather model emulator ACE2, focusing on how the stratosphere and upper troposphere influence winter storms. Understanding the drivers of winter storminess is essential for improving sub-seasonal prediction skill in regions strongly affected by extratropical cyclones. Using ERA5 reanalysis data (1940–2024), we built a storminess index based on storm event frequency, examined its relationship with large-scale atmospheric fields, and explored its predictability at seasonal timescales.

We aim to predict North Sea storminess using two approaches: one based on the ACE2 climate emulator and another on the Random Forest machine learning algorithm. For the ACE2 model, we used modified air temperature and zonal and meridional wind patterns at 70 hPa as predictors, which were imposed as initial conditions on the 1st of each winter month, and tested changes in storminess over the ensuing weeks and months of the winter season. For the Random Forest regression model, we used monthly means of air temperature, zonal wind at 70 hPa, and geopotential height at 200 hPa as predictors to predict storminess in the following months. The ACE2 simulations show that by modifying the stratospheric initial conditions on 1st December, we can increase the emulated mean January surface wind speeds by about 0.5–3 ms^{-1} across much of the North Sea. Similar sensitivity emulations initialised at the start of other months, e.g. November 1st, failed to produce a meaningful response in the ensuing month. This suggests a dynamic link between early-winter stratospheric conditions and increased mid-winter surface storminess.

The Random Forest Regression model was applied after dimensionality reduction using Principal Components Analysis (PCA). The best results were obtained by predicting January storminess from the mean December fields, yielding a correlation between prediction and target of approximately 0.55–0.60. For other month pairs, the correlation ranges from 0.20 to 0.36 for November–to-December and January–to-February predictions, but it becomes negative (–0.44 to –0.05) for October–to-November and February–to-March predictions.

This seasonal predictability pattern, derived from both the ACE2 emulations and the Random Forest model, follows the seasonal cycle of the polar vortex's average intensity. The circumpolar westerly jet strengthens from autumn and peaks in winter, when predictability is highest. This higher skill is likely linked to stronger stratosphere–troposphere coupling between November and January, as polar vortex anomalies develop and begin to descend toward the surface. Both indicate that the seasonal predictability of storminess peaks in mid-winter, with a predictability lead time of about 4 to 6 weeks. It fades for the earlier and late winter periods.

https://doi.org/10.5194/egusphere-2026-1225
Preprint. Discussion started: 9 March 2026

Overall, this research shows that stratospheric conditions play an essential role in shaping North Sea winter storminess and that machine learning methods can improve sub-seasonal predictions in this region.

1 Introduction

Seasonal climate prediction typically focuses on forecasting mean seasonal values a few months ahead, using either ensembles of initialised simulations from Earth System models or predictors identified for statistical prediction schemes. Although forecasts of seasonal means can undoubtedly be very important for many economic and societal sectors, probabilistic predictions of just the frequency of specific types of extremes can also be beneficial and perhaps easier, as they focus on a specific range of the probability distribution. The North Sea, a shallow sea in Western Europe connected to the North Atlantic, is strongly exposed to winter wind extremes, which affect shipping and impact the coast, causing storm surges, coastal flooding, and coastal erosion (Donat et al., 2011; Feser et al., 2014; Schade et al., 2025). In this study, we explore the possibility of predicting the stormy character of the winter months in the North Sea with a lead time of a few months.

Surface winds in wintertime in the North Atlantic and the North Sea are statistically linked to the North Atlantic Oscillation (NAO), a dominant pattern of interannual climate variability in the North Atlantic sector that displays well-known teleconnections to near-surface temperature, sea-surface temperature (SST) and precipitation (Hurrell et al., 2003; McKenna and Maycock, 2022). Essentially, the NAO describes the strength of the mid-latitude zonal atmospheric circulation over the North Atlantic, as summarised by the seasonal mean air pressure differences between the Azores and Iceland (Hurrell et al., 2003), although other indices based on Principal Component Analysis of the North Atlantic sea level pressure field are also commonly used (Pinto and Raible, 2011).

Due to its dominant role in interannual winter climate variability in the North Atlantic-Western European sector, several studies have sought to identify seasonal precursors of the NAO state. Some of these studies have focused on the role of Tropical Atlantic (Wang et al., 2017; Sung et al., 2013) and Tropical Pacific SST (Sung et al., 2013). Regarding the state of the Tropical Pacific, previous studies have found that warmer temperatures, corresponding to an El Niño phase, tend to be associated with a weaker NAO, colder North European winters, and wetter Western Mediterranean conditions. In contrast, the opposite phase, La Niña, is statistically associated with a stronger NAO, with warmer North European winters and drier Western Mediterranean (Brönnimann, 2007). However, these links appear to be weak, non-stationary, and non-linear, and may also be modulated by the state of the Pacific Decadal Oscillation (Gershunov and Barnett, 1998). For example, the European winter 2025-2026, with a predominant La Niña state in the Tropical Pacific and a negative NAO, illustrates a clear counterexample. Other sources of predictability identified in model studies are the extent of Arctic sea-ice cover and the Quasi-Biennial Oscillation. Scaife et al. (2014) use a new long-range forecast system to show that winter climate over the North Atlantic region, specifically the NAO, storminess, temperature, and wind speed, may now be highly predictable months in advance. However, the analysis also reveals that although forecast skill is significant, some key sources of predictability remain underrepresented, suggesting potential to improve long-range climate forecasting.

https://doi.org/10.5194/egusphere-2026-1225
Preprint. Discussion started: 9 March 2026

The NAO is more directly connected to the Arctic Polar Vortex in the lower stratosphere (Kidston et al., 2015), with a stronger winter vortex and a stronger winter NAO tending to occur simultaneously on seasonal timescales. The normal westward zonal flow of the lower stratospheric winds within the polar vortex can be disrupted by Sudden Stratospheric Warming (SSW) events. SSW are intraseasonal events caused by the intrusion of vertically propagating tropospheric gravity waves into the stratosphere (Baldwin et al., 2020), which modify the vertical temperature profile and dynamically disrupt the lower stratospheric zonal flow. Kidston et al. (2015) explains how variations in the strength of the stratospheric polar vortex strongly influence the tropospheric jet stream, storm tracks, and extreme surface weather. When the vortex weakens, especially during strong SSWs, the tropospheric jet shifts towards the equator, increasing the likelihood of cold outbreaks, blocking, and extreme winter weather over Europe and North America. When the vortex strengthens, the jet shifts poleward, enhancing surface winds at mid latitudes. These downward impacts occur because wave-driven disturbances in the stratosphere modify mass, pressure, and eddy momentum in the troposphere, producing consistent surface responses from weekly to decadal timescales. That study highlights that stratospheric variability also affects the ocean and provides significant skill for subseasonal-to-seasonal forecasts, making an accurate representation of the stratosphere essential for reliable climate predictions and projections.

To this brief picture of possible precursors of the seasonal mean NAO, one should also keep in mind that the phase of the Tropical Pacific SST also influences the Arctic polar vortex, and that this influence can be complex. For instance, it has been found that during *both* phases of ENSO, the frequency of SSW is higher than during neutral phases. This makes it more difficult to identify the remote SST precursor of extreme winds in the North Sea, as the linkage is likely to occur through several pathways and be strongly nonlinear.

With this background, this study aims to assess the predictability of stormy winter seasons in the North Sea, a relatively small but economically important region for Western Europe. Storm surges cause a significant rise in coastal water levels, which can have substantial socio-economic consequences and, in extreme cases, may even result in fatalities. Furthermore, these extreme water levels, in combination with strong winds and long-lasting precipitation events, can severely impact onshore and offshore transport systems and their infrastructure (Kew et al., 2013; Schade, 2017). Winter storms are among the most damaging climate hazards in northwestern Europe, and the North Sea region is particularly exposed due to its frequent extratropical cyclones and strong winds (Donat et al., 2011; Feser et al., 2014). A better understanding of these storms and the ability to predict them a season in advance are crucial for coastal protection, offshore wind planning, and the management of climate-related risks.

A study by Krieger et al. (2024) has shown that seasonal forecasts of German Bight storm activity using the hindcast system of the Earth System model MPI-ESM can be improved by subsampling the ensemble of simulations according to their individual agreement between the simulated and observed air temperatures at the 70 hPa geopotential height level in September, two months before the target prediction month. The initial predictive power of the whole ensemble is weak due to a very large spread. Using 70 hPa temperature anomalies (September) and 500 hPa geopotential height anomalies (November) as filtering criteria, the authors select ensemble members that agree with a first-guess forecast. This subselected ensemble significantly boosts prediction skill by better capturing large-scale atmospheric patterns. Other studies have examined storm predictability using various methods, including dynamical modelling (Xie et al., 2021; Tian et al., 2024; Gao et al., 2024; Pu and Kalnay,

https://doi.org/10.5194/egusphere-2026-1225
Preprint. Discussion started: 9 March 2026

2018), mathematical modelling (Tian et al., 2024), data-driven machine learning (Gao et al., 2024), and dynamical modelling and data assimilation (Pu and Kalnay, 2018).

In our study, we employ two approaches to explore the predictability of stormy winter seasons in the North Sea. We define stormy days as days in which the daily mean wind exceeds a high percentile of the climatological probability distribution. Stormy seasons are those with a higher frequency of stormy days (see section 2). One prediction methodology used here is Random Forest, a machine-learning method for categorical classification or predicting a response variable from several predictors (Breiman, 2001). The technique can be augmented with Random Forest Regression (RFR), which increases the number of categories to cover a given output range using a specified number of bins. The method can capture strongly non-linear links between the predictor and the predictand. In our case, the predictand is the number of exceedances of extreme daily wind, and the predictors may include the temperature field in the lower stratosphere from the previous season or earlier months, although other predictors were also tested.

The second method is based on the, to our knowledge, first application of the atmospheric emulator ACE2 in a long-range weather forecast setting (Watt-Meyer et al., 2025). The ACE2 emulator is a machine-learning-based emulator of atmospheric dynamics that can be trained using reanalysis data or data from a climate simulation. This emulator has been shown to replicate important characteristics of global atmospheric dynamics and its response to tropical SST forcing (see section 3.2). The main characteristics of the atmospheric circulation in the Northern Hemisphere are also well replicated (Bellinghausen et al., 2026). In our study, we utilised the ACE2 model in sensitivity runs of two months' length, in which the initial conditions are modified to mimic patterns of lower stratospheric warming or cooling and a strong or weak lower stratospheric polar vortex. The simulated North Sea extreme winds are then compared with those simulated in runs initialised with observed initial conditions. This approach follows a similar concept to a recent idealised modelling study by Mouallem et al. (2025), in which controlled changes are applied to the stratospheric circulation to isolate how such perturbations affect the troposphere, without attempting to reproduce the full evolution of SSW events. To trigger SSWs, their model is perturbed using an idealised, moving topographic forcing that generates vertically propagating planetary waves.

After this introduction, the paper describes the data sets and briefly summarises the structure of the ACE2 emulator. It then proceeds to analyse the spatio-temporal persistence of stormy winter months in the North Sea, concluding that SST and other persistent boundary conditions are unlikely predictors of stormy months in this region. Section 3 then presents the main statistical analysis to identify suitable predictors, followed by the prediction scheme based on Random Forest (section 4.2) and the sensitivity analysis using the ACE2 emulator. The paper is closed by a summary and conclusion (section 6).

2 Methods

2.1 Dataset

Atmospheric and oceanic variables for the period 1940–2024 were obtained from the ERA5 reanalysis, the fifth-generation global climate dataset produced by the European Centre for Medium-Range Weather Forecasts (ECMWF) (Hersbach et al., 2020). The ERA5 dataset is produced by reconciling historical observational data with atmospheric physics encapsulated in a

https://doi.org/10.5194/egusphere-2026-1225
Preprint. Discussion started: 9 March 2026

weather prediction model to ensure a continuous and consistent global record across all variables. The data were retrieved at a horizontal resolution of $0.25° \times 0.25°$ (approximately 31 km) on 137 atmospheric levels, extending from the surface to 0.01 hPa. In this study, we analysed monthly averages of geopotential height (200 hPa), air temperature (70 hPa), and zonal wind (70 hPa), as well as daily 10-meter wind speeds (Hersbach et al., 2020).

2.2 Definition of storminess

To calculate the number of stormy days in each month, we first obtained the zonal and meridional daily wind speeds at 10 meters from the ERA5 reanalysis for a particular calendar month. We then calculated daily wind speeds from these values and determined the climatological 90th percentile for each grid cell. We selected the 90th percentile to ensure sufficient sample size for robust statistical analysis. We then calculated the number of days on which wind speed exceeded the 90th percentile in each month and defined these counts as stormy days. As representative of the North Sea, we chose one grid cell in the North Sea (Fig. 1). As illustrated by the spatial map showing the temporal correlation between the storminess in the chosen grid cell and all other grid cells in the North Sea (Figure 2), the frequency of January stormy days in this grid cell is highly correlated with the rest of the North Sea, justifying its use as a representative index for the region.

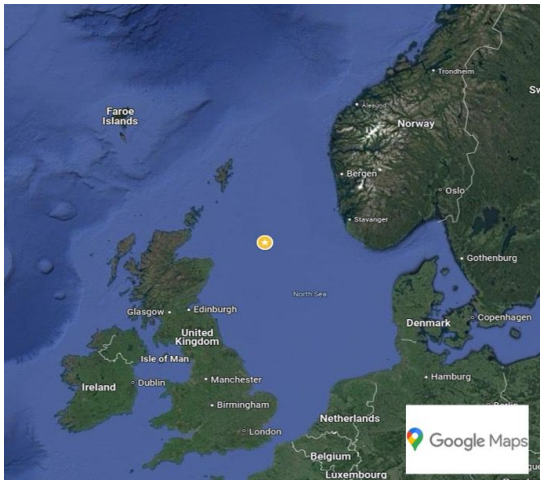

Figure 1. Map of the selected grid cell in the North Sea (1°E, 58°N). Map data: ©2025 Google

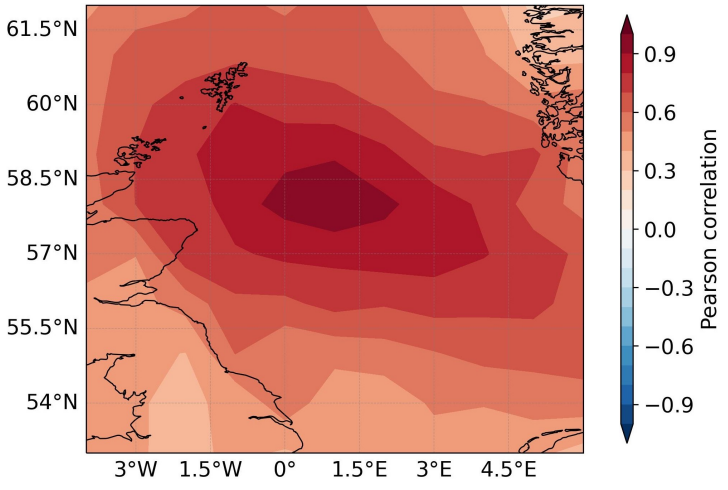

Figure 2. Correlation between January storm counts (1940–2024) at each North Sea grid point and the storm count time series at the reference location (1°E, 58°N).

3 Preliminary considerations on possible predictors: spatiotemporal persistence of storm frequency

The first preliminary question we explored was how persistent over time the stormy character of a particular month is, e.g., whether a stormy January tends to be followed by a stormy February or preceded by a stormy December. Another related

https://doi.org/10.5194/egusphere-2026-1225
Preprint. Discussion started: 9 March 2026

question is the spatial coherence of storminess. Figure 1 indicates that our chosen grid cell is representative of the North Sea, but it would be helpful to know how large the area of coherence is. These questions can provide information about the possible large-scale predictors of storminess.

It turns out that the temporal persistence of the monthly number of stormy days is very low. The cross-correlations between the number of stormy days in the winter months, belonging to the same winter season, in the selected North Sea grid cell are shown in Table 1. Similarly, the global map of correlations between the number of January stormy days in the North Sea grid cell with all other grid cells shows that the coherence length is rather short, with high correlations located only in the region close to the basis grid cell.

Month	Dec	Jan	Feb	Mar
Dec	1.00	-0.15	-0.04	0.20
Jan	-0.15	1.00	0.03	0.05
Feb	-0.04	0.03	1.00	0.26
Mar	0.20	0.05	0.26	1.00

Table 1. Pearson correlation matrix of monthly storm counts (December–March) at the reference North Sea grid point. Correlations are computed between annual storm-count time series for each winter month over the analysis period (1940-2024).

This short spatio-temporal coherence is not compatible with a relevant role for large-scale SST patterns, since SSTs anomalies are persistent over periods of several months (Kushnir, 1994). If SSTs were a relevant predictor of North Sea storminess, a stormy January would tend to be preceded by a stormy December and followed by a stormy February. This is not what we observe.

By a similar reasoning, large-scale patterns of remote SST anomalies, e.g., in the Tropical Pacific or the North Atlantic, would plausibly drive storminess over large areas in Europe and perhaps beyond the North Atlantic. The possible mechanisms for atmospheric wave trains excited by SST anomalies would modulate storminess at continental scales, not just in the North Sea.

For these reasons, we turned our attention to shorter-lived atmospheric precursors of storminess. Among those, lower stratospheric temperatures and the occurrence of SSW have been suggested as drivers of perturbed atmospheric dynamics in this region (Domeisen, 2019; Baldwin et al., 2020). However, the relatively small-scale coherence of storminess suggests that storminess in the North Sea would be driven by particular, likely also regionally constrained, configurations of SSWs and lower-stratospheric winds, rather than solely by circumpolar dynamics of the polar vortex. Our hypothesis is therefore that the state of the circumpolar polar vortex may be a precondition for storminess in the North Sea, but that this preconditioning would need to be additionally modulated by more regional dynamics that affect the North Sea and not other adjacent regions.

https://doi.org/10.5194/egusphere-2026-1225
Preprint. Discussion started: 9 March 2026

3.1 Precursors of stormy Januaries

To identify the configuration of the precursors, stratospheric temperature, and stratospheric winds that lead to more stormy Januaries in the North Sea, we selected the five stormiest Januaries and the five calmest (no storm) Januaries within the study period. For each case, we calculated the average air temperature and zonal and meridional wind anomalies (deviations from the climatological December mean) at 70 hPa in December, using daily ERA5 data. This allowed us to examine how the stratospheric state in December varies with the storminess of the following January.

The results show that the stratospheric air temperature tends to be significantly cooler already in the Decembers preceding stormier Januaries (Fig. 3). This supports previous studies suggesting that stratospheric air temperature anomalies are key precursors of winter storm activity (Krieger et al., 2024).

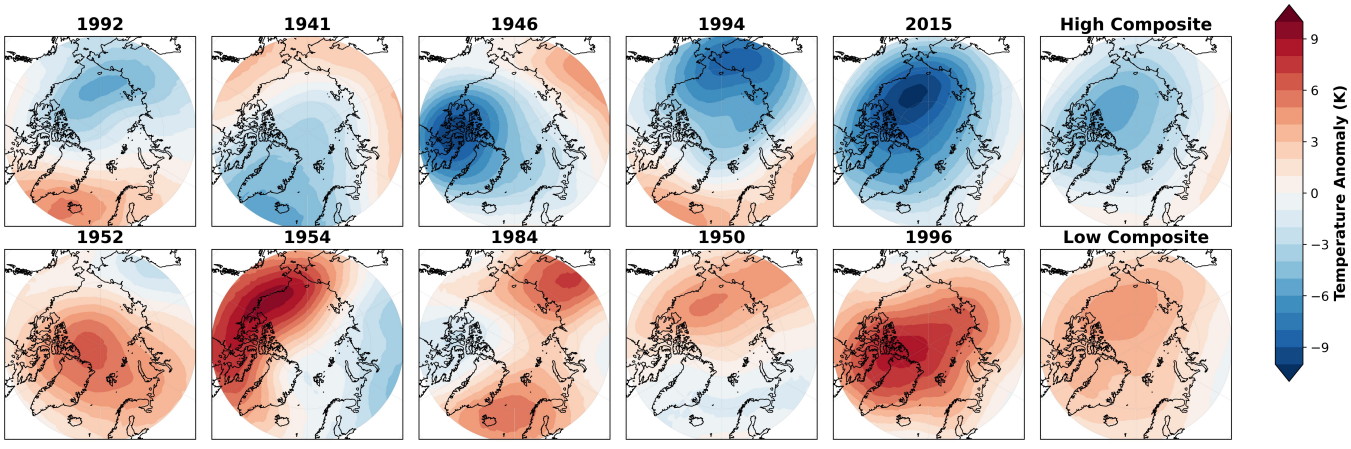

Figure 3. Temporal mean of air temperature at 70 hPa in the Decembers prior to Januaries with a high (upper row) and low (lower row) number of storms.

A similar analysis was performed for the anomalies of the stratospheric zonal and meridional wind components at 70 hPa. Specifically, we computed the corresponding anomalies for the Decembers preceding the Januaries with the five highest and five lowest storminess values. We found that monthly mean zonal wind speeds in the stratosphere are stronger during the Decembers preceding stormier Januaries (Figs. 4, 5), consistent with enhanced stratospheric westerlies and a stronger polar vortex.

We also include the December monthly mean of geopotential height anomalies at 200 hPa, which has a strong link to wind speed and affects the North Atlantic Oscillation (NAO). Upper-level troughs and ridges are associated with cyclonic and anticyclonic flow, respectively. A trough corresponds to a region of lower geopotential height and stronger winds on its eastern flank. In contrast, a ridge corresponds to higher geopotential height and weaker winds on its western flank (Schemm et al., 2020).

https://doi.org/10.5194/egusphere-2026-1225
Preprint. Discussion started: 9 March 2026

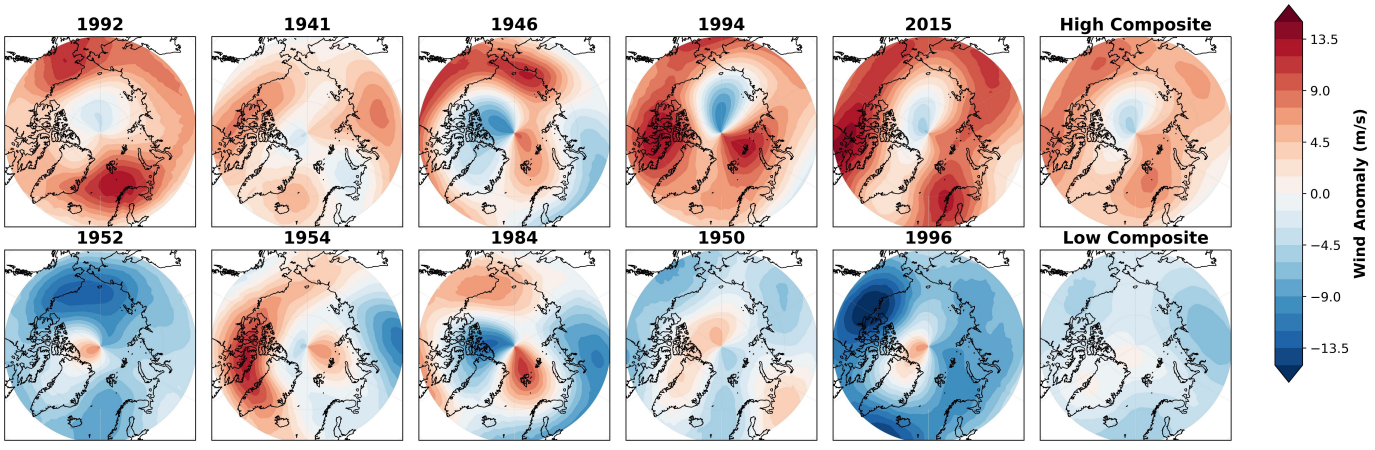

Figure 4. Temporal mean of zonal wind at 70 hPa in the five Decembers preceding the five Januaries with high storm activity (top row) and low storm activity (bottom row) in the North Sea.

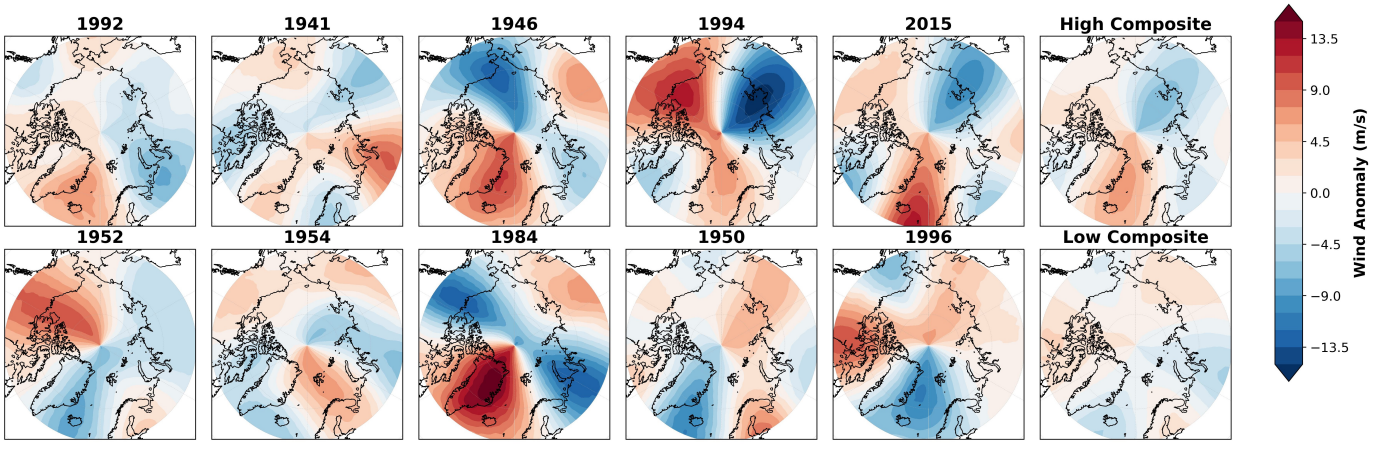

Figure 5. Same as Figure 4 but for the meridional wind at 70 hPa height.

These identified patterns of average anomalies in the Decembers preceding Januaries with the highest frequency of North Sea stormy days were used to modify the initial conditions in an ensemble of simulations with the atmospheric emulator ACE2, starting on December 1st and running for two months. The output was then compared with a corresponding ensemble of simulations started with observed initial conditions on December 1st. The results are described in the next sections.

A similar procedure was applied to the other two winter months, December and February, but, as discussed later, the signal and predictability were weaker than in January.

https://doi.org/10.5194/egusphere-2026-1225
Preprint. Discussion started: 9 March 2026

3.2 ACE2: ML-based atmospheric model

We used the ACE2 (AI2 Climate Emulator, version 2) model to emulate atmospheric variability over the last 80 years. ACE2 is an autoregressive machine learning model that simulates atmospheric dynamics over timescales ranging from days to decades. It has around 450 million parameters and runs with a 6-hour time step, 1° horizontal resolution, and eight terrain-following vertical layers. It is trained to predict two 6-hour steps ahead and uses a Spherical Fourier Neural Operator (SFNO), which is designed for data defined on a sphere. It requires prescribed 6-hourly fields of external forcings for surface temperature, top-of-atmosphere solar insolation, and CO_2 concentrations. An important feature of ACE2 is that it conserves global dry air mass and moisture exactly, allowing it to run stably for very long periods, up to thousands of years, without developing artificial drift (Watt-Meyer et al., 2025).

Compared with the first ACE version, ACE2 offers three significant improvements: it includes CO_2 as a forcing, reproduces historical trends over the past 80 years, and applies physical corrections during inference to preserve conservation laws. The model outputs standard meteorological fields: winds, temperature, humidity at 8 atmospheric levels; precipitation; near-surface temperature; surface pressure; and radiative fluxes at the surface. During training, some diagnostic variables are weighted differently based on their behaviour, and additional corrections help ensure that precipitation and evaporation remain consistent with changes in atmospheric moisture.

The ACE2 version used here was previously trained by its authors on ERA5 data (Watt-Meyer et al., 2025) (a previous version was trained on the output of the global atmospheric model SHiELD (Watt-Meyer et al., 2023)). It can generate realistic features, such as the Madden-Julian Oscillation and tropical cyclones, the ENSO cycle, and capture long-term trends. Despite being a machine-learning model, ACE2 can produce stable, physically meaningful climate simulations at a much lower computational cost than traditional climate models (Watt-Meyer et al., 2025).

In a typical simulation with the ACE2 model, the model is initialised with a snapshot of initial conditions and fields of external forcings covering the simulation period. Here, we will use the ACE2 model to conduct two sets of simulations. Within each set, each simulation covers selected two-month periods, starting on December 1st and ending on January 31st. The initial conditions for this set are taken from the ERA5 reanalysis. In the second set, the initial conditions on December 1st are perturbed using modified fields of air temperature and the two wind components at 70 hPa.

Note that the temporal evolution of the unperturbed set will rapidly diverge, after a few days, from the observed evolution encapsulated in ERA5, since the ACE2 model is not run with any data assimilation. In this sense, it mimics an initialised free-running weather prediction model. However, using these simulations, we explore whether perturbed surface initial conditions can still drive the ACE2 model to produce stronger or weaker winds in the North Sea region several weeks after initialisation.

We used ACE2 because it provides a tool for simulating atmospheric variability at high temporal resolution while remaining computationally very efficient. Our focus was on understanding stratospheric forcing of the troposphere, primarily through stratospheric air temperature anomalies, and ACE2 enabled quick, flexible emulation of these dynamics. We were able to generate simulations efficiently and repeatedly, which was critical for testing different configurations and initial conditions, and for averaging across ensemble members to extract robust signals from noisy atmospheric data.

https://doi.org/10.5194/egusphere-2026-1225
Preprint. Discussion started: 9 March 2026

3.2.1 ACE2: Preprocessing

We start this subsection by explaining how the ACE2 initial conditions were prepared. The initial states provided by the ACE2 package (Ai2, 2025) stem from ERA5, and we selected December months for which the following January was calm (zero to one storms). We ran ACE2 for multiple Decembers associated with low January storminess, each with distinct initial conditions, and present six representative cases. These years were selected because their subsequent Januaries showed very low storm activity in ERA5 (zero to one storm), allowing the influence of the altered initial conditions to stand out more clearly. The initial condition is set for December 1st, and the model is then run for 60 days. For each case, we first run the model starting on December 1st, 00 UTC using the unmodified initial condition (the "control" ensemble). Then we rerun it with modified initial conditions (the "perturbed" ensemble). By comparing the two runs, we can see whether the changes we introduce in the stratosphere lead to stronger surface winds.

Next, we describe how the initial conditions were modified. The anomaly maps of air temperature and zonal and meridional wind shown in Figures 3, 4, and 5 reveal clear stratospheric circulation patterns. Based on these patterns, we focus on monthly mean anomalies from December 2015, as Figure 3 shows a relatively cool polar stratosphere at that time. Such conditions are commonly associated with a positive NAO–like circulation and enhanced winter storm activity (Domeisen, 2019; Domeisen and Butler, 2020; Charlton-Perez et al., 2018). The air temperature and wind fields at 70 hPa are used to construct the "polar mask." This mask is then added to the corresponding variables in the unperturbed ACE2 initial conditions to impose a modified stratospheric state. The model is subsequently rerun for two months, and the resulting changes in the simulated atmospheric evolution are analysed.

3.3 Random Forest Regression model

To support the results obtained with the ACE2 model, we use another established ML method, namely Random Forest Regression (RFR), to establish a data-driven month-to-month predictive scheme that takes as input the monthly means of stratospheric fields of 70 hPa air temperature and winds to produce a forecast of the number of stormy days in the following month. RFR is an ensemble learning method that combines many decision trees to produce a single prediction. Each tree is trained on a random subset of the data and a random subset of the predictors, reducing the influence of noise and improving the stability of the final estimate. The method was introduced by Breiman (2001) and has since become widely used in climate science because it can recover complex, nonlinear relationships without requiring strong assumptions about the data structure. It also handles large predictor sets, spatial correlations, and predictor interactions well, which is especially relevant for atmospheric fields (Gagne II et al., 2019).

In this study, we used RFR to examine how the state of the stratosphere within the polar region in December relates to storminess in the North Sea the following January (the Dec–Jan relationship). We then applied the same approach to other month pairs (Oct–Nov, Nov–Dec, Jan–Feb, and Feb–Mar) to examine how this relationship evolves across the season. The predictors consist of monthly mean fields of air temperature at 70 hPa, zonal wind at 70 hPa, and geopotential height at 200 hPa from the ERA5 reanalysis spanning from 1940 to 2024, within the polar region (60°N to 90°N). For each year, the gridded

https://doi.org/10.5194/egusphere-2026-1225
Preprint. Discussion started: 9 March 2026

fields were flattened into feature vectors, so each December became a single sample representing the spatial pattern of the stratosphere. The predictand is the number of stormy days observed in our selected North Sea grid cell during the following January.

3.3.1 RFR: Preprocessing

To construct the dataset used for predicting January storminess in the North Sea, we first derived a storm index from ERA5 daily 10-meter wind data. The total number of such days per January forms the annual storm index used as the predictand.

Three dynamical and thermodynamical predictor fields from ERA5 were used: air temperature at 70 hPa, geopotential height at 200 hPa, and zonal wind at 70 hPa. Each dataset was converted to a -180 ° to 180° longitude system, sorted, and spatially restricted to the Arctic domain (60°N to 90°N). The latitude and longitude dimensions were then flattened so that each December map becomes a single one-dimensional feature vector.

Finally, all predictor fields were temporally aligned with the storm index, and years with missing data were removed to maintain consistency across variables. The resulting arrays were stored in a compressed archive to ensure reproducibility. For the machine-learning experiments, the available years were randomly divided into a training set (70%) and an independent test set (30%). The same random split was used for all experiments to ensure consistency across different predictor configurations. No cross-validation was applied. Predictor fields were standardised using a StandardScaler, concatenated, and reduced in dimensionality using Principal Component Analysis (PCA) prior to training the Random Forest models.

4 Results

4.1 ACE2 Model output

We ran ACE2 for multiple Decembers associated with low January storminess, each with distinct initial conditions, and present six representative cases. Figure 6 illustrates the results for the simulations started on December 1st, 1948, 1949, 1950, 2000, 2001, and 2020. We run the model for 60 days and calculate the difference of mean wind speed (perturbed run - control run) response from 7 December to 31 January (Fig. 6). Over several years, including 1948, 1949, 1950, 2000, and 2020, we observe an increase in surface wind of 0.5–3 ms^{-1} following the introduction of the stratospheric perturbation.

Although these years, such as 1948, 1949, 1950, 2000, and 2020, were followed by relatively non-stormy Januaries in the observations, their responses to the perturbation differ. Therefore, we also present an example of a slightly different situation for the simulation started in December 2001 (Fig. 6). After adding the "polar mask" to the initial condition and running the model for two months, surface wind speeds do not seem to increase across the entire region. We only see a modest increase, mainly south of Norway in the North Sea. This suggests that the storminess response does not depend solely on the imposed stratospheric perturbation. There are also other contributing factors, but they are not addressed in this study.

https://doi.org/10.5194/egusphere-2026-1225
Preprint. Discussion started: 9 March 2026

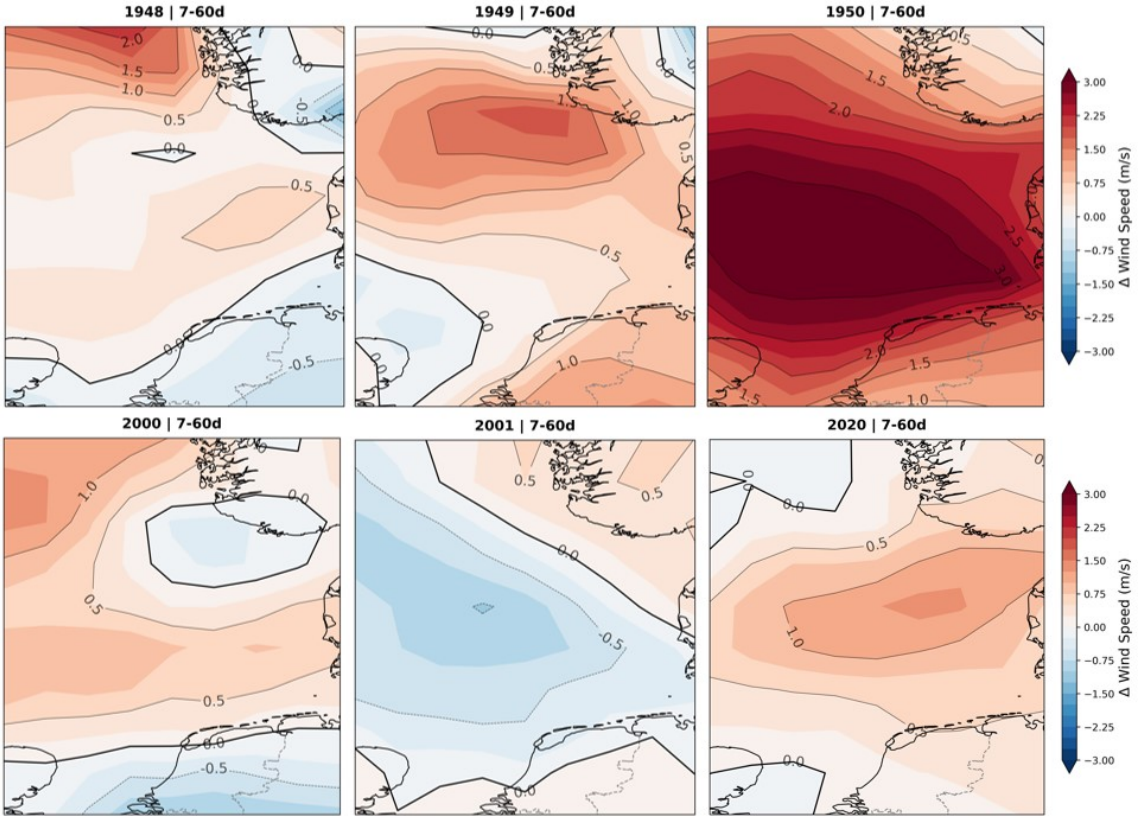

Figure 6. Temporal mean of 10m wind speed response from ACE2 simulation (perturbed - controlled) for days 7–60 following initialisation. Shown are the difference fields for the cases December of 1948, 1949, 1950, 2000, 2001, and 2020. Warm colours indicate stronger near-surface winds in the perturbed run, while cool colours show reduced winds.

4.2 Random Forest Regression model output

The model evaluation shows that the Random Forest captures a meaningful portion of the relationship between December atmospheric conditions and the number of storms observed in the North Sea during the following January (Figures 7, 8). Across all tested configurations, the best-performing setups yield correlations in the range 0.55–0.60. This indicates that December's large-scale atmospheric conditions account for nearly one-third of the following month's North Sea storminess.

The scatter plot (Fig. 8) shows the model behaviour on the test set (30% of the data), which is much smaller and therefore noisier. The correlation of 0.56 and the shallow slope of the red regression line indicate that the model correctly captures the direction of the variability but tends to underestimate and sometimes overestimate extreme values. Nevertheless, the points show that the model rarely fails dramatically; predicted values remain within a consistent band and follow the general trend of the observations. This picture becomes clearer in the time-series comparison (Fig. 7), where observed and predicted storminess

https://doi.org/10.5194/egusphere-2026-1225
Preprint. Discussion started: 9 March 2026

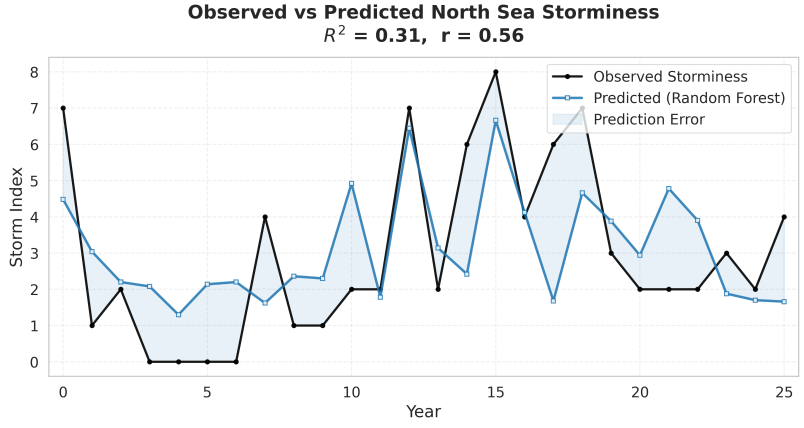

Figure 7. Comparison between observed and Random Forest predicted North Sea storminess (1940–2024). Time series of observed (black-test set) and predicted (blue) storm indices.

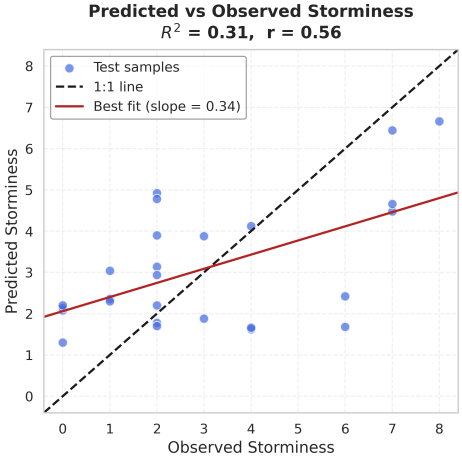

Figure 8. Scatterplot of observed vs predicted storminess for the test set, illustrating model skill.

evolve in a broadly similar manner. Many peaks and troughs align, particularly in the middle to late part of the test period, indicating that the model reproduces the temporal structure of stormy and calm winters.

Understanding why the model achieves this level of skill requires examining the contributions of the predictors. The feature importance figure 9 indicates that PC1 (the first principal component, which captures the dominant pattern of variability in the dataset) and PC5 account for most of the predictive power, followed by PC3, PC2, and several others with smaller but still meaningful contributions.

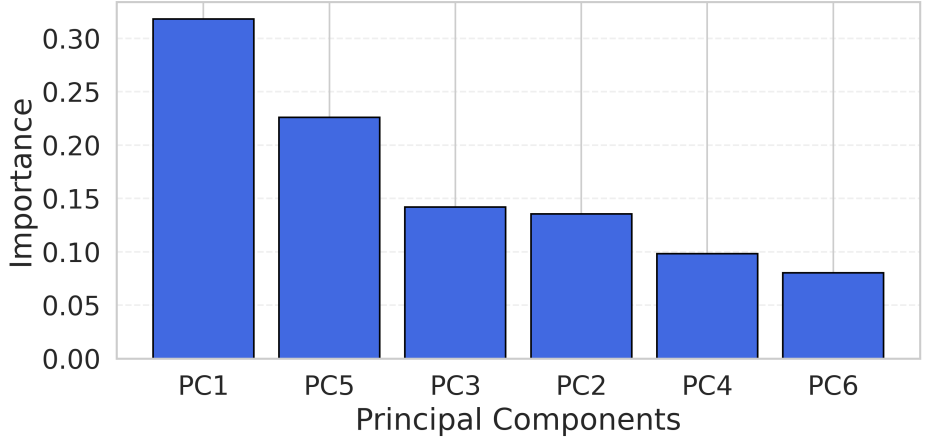

Figure 9. Importance of Principal Components Used as Predictors in the Random Forest Model

https://doi.org/10.5194/egusphere-2026-1225
Preprint. Discussion started: 9 March 2026

To interpret these physically, the PCs' loading maps are essential (Fig. 10). They reveal coherent Arctic-wide structures in geopotential height at 200 hPa (top row), zonal wind (middle row) and temperature at 70 hPa (bottom row). A PC loading is the weight that shows how strongly a variable contributes to a principal component.

All three fields for PC1 exhibit patterns associated with the strength of the polar vortex. For geopotential height, PC1 shows a broad region of positive PC loading centred over the polar cap, consistent with an intensified vortex. The temperature field at 70 hPa shows positive PC loading across the Arctic, indicating enhanced stratospheric stability, which is also linked to a strong, stable vortex above. The zonal wind pattern mirrors this structure, with strong positive westerly anomalies extending across the high latitudes. These three patterns together reflect a dynamically consistent state of the stratosphere in December. PC5, PC3 and PC2, on the other hand, show asymmetric structures that include a distorted polar vortex. According to Zhang et al. (2024), when the polar vortex is weak, the atmosphere becomes less active and stormier, and weather systems that usually transport air and energy weaken, making it easier for high-pressure systems to form and persist. As a result, more blocking occurs over Greenland, as seen in PC5.

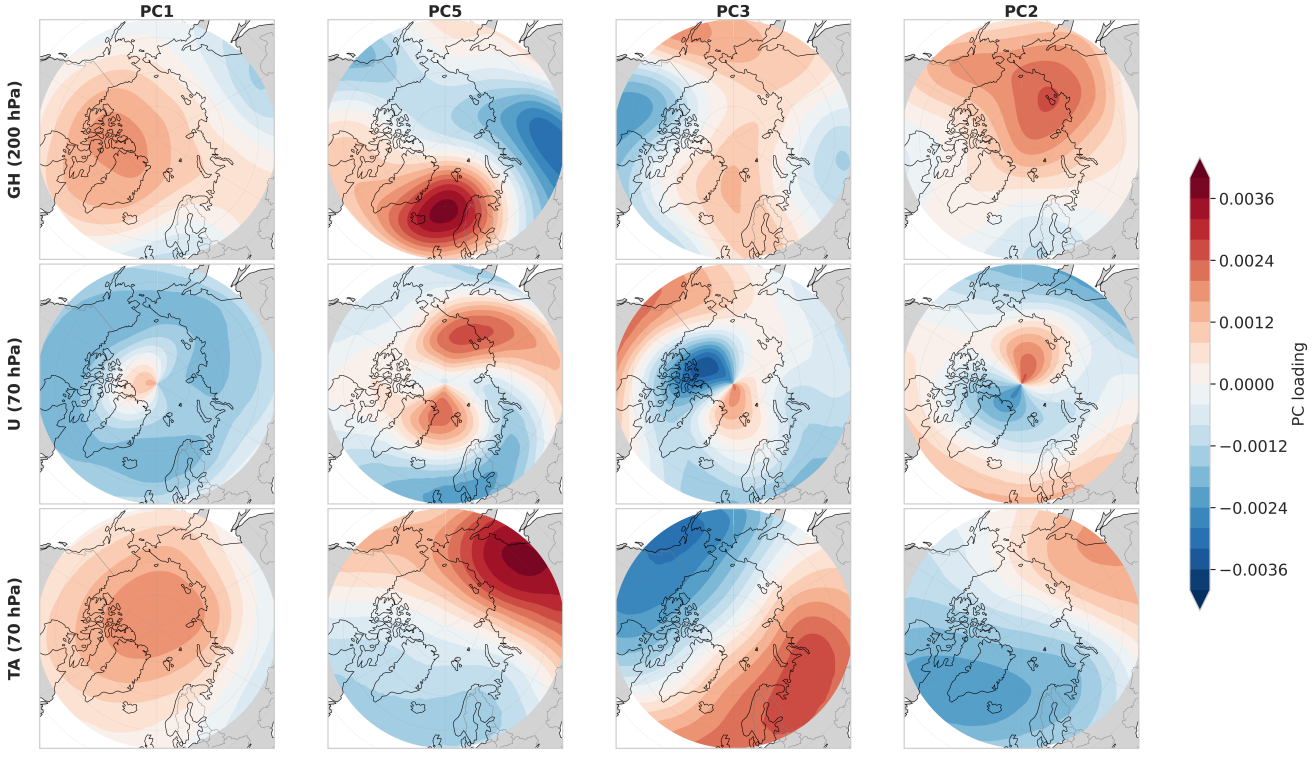

Figure 10. Spatial patterns of the principal component (PC1, PC5, PC3 and PC2) of the December mean fields derived from ERA5 (1940–2024) for geopotential height at 200 hPa (GH), air temperature at 70 hPa (TA), and zonal wind at 70 hPa (U).

Because the polar vortex is a known driver of the North Atlantic circulation in the coming weeks, these PC patterns provide a physically meaningful basis for predictability. A strong vortex in December often promotes a stronger, more zonal jet stream

https://doi.org/10.5194/egusphere-2026-1225
Preprint. Discussion started: 9 March 2026

in January, increasing the likelihood of frequent storms entering the North Sea region (discussed in the introduction 1). This is precisely the kind of signal the model is taking into account. In short, the predictors primarily represent the large-scale Arctic dynamical environment, particularly the state of the stratosphere and its coupling with the North Atlantic jet.

4.2.1 Predictability within different months

In the previous subsection, we focused only on the predictability between the predictors from December and the predictand in January. Using the same methodological setup as for the Dec-Jan pair, we now investigate the predictability using the Random Forest approach for different predictor-predictand month pairs as stated in Table 2.

Months	R^2	Corr (r)	RMSE
Oct–Nov	-0.39 to -0.61	-0.31 to -0.05	∼2.5
Nov–Dec	-0.1 to 0.1	∼0.31	∼1.6
Dec–Jan	0.29 to 0.31	0.55 to 0.60	∼1.9
Jan–Feb	-0.05 to 0.11	0.2 to 0.36	∼1.7
Feb–Mar	-0.30 to -0.35	-0.28 to -0.44	∼2.5

Table 2. Summary of the Random Forest model performance metrics for different predictor–predictand month pairs. The first month is the predictor month, and the second month is the predictand month. The correlations are calculated between predictions and target in a reserved independent data set not used for the training of the RF methodology, in a similar fashion as for the December-January case.

We observe that the correlation reaches negative numbers for October-November and February-March. Evidently, we observe higher correlations during the months of November-December, December-January, and January-February. This can be related to the formation of the polar vortex, which forms in autumn (September to November), peaks in winter (December to February), and breaks down in spring (March onwards) (Domeisen and Butler, 2020). We observe that predictability is higher during winter than in autumn or spring. So there is a high chance that the higher predictability comes from the relationship between the polar vortex in the stratosphere and its effects on Earth's surface, because the strongest stratosphere–troposphere coupling occurs between November and January, when stratospheric circulation anomalies persist and begin descending toward the surface (Kidston et al., 2015). The downward influence of polar vortex anomalies on the lower stratosphere can modulate the tropospheric circulation. In the Northern Hemisphere (NH), SSWs occur on average every other year and often lead to persistent blocking over Greenland associated with the negative phase of NAO (Charlton-Perez et al., 2018; Domeisen, 2019), altering surface weather for weeks to months (Limpasuvan et al., 2005). A strengthening of the stratospheric polar vortex, on the other hand, tends to exert an opposing downward influence on the NAO, towards its positive phase (Domeisen and Butler, 2020).

https://doi.org/10.5194/egusphere-2026-1225
Preprint. Discussion started: 9 March 2026

5 Limitations and future work

While this study highlights new connections between stratospheric conditions and North Sea storminess, several limitations should be acknowledged. The storminess metric is based solely on surface wind speed and does not include sea-level pressure or precipitation. In addition, storminess is counted in a single grid cell in the North Sea, which simplifies the regional wind structure. The ERA5 datasets also have weaknesses: ERA5 dataset uses a data assimilation scheme to constrain its state to remain close to observations, fields such as the surface precipitation rate and radiative fluxes are not constrained and exhibit non-trivial biases relative to satellite and station observations (Hersbach et al., 2020; Urraca et al., 2018). ERA5 is also known to underestimate strong offshore winds relative to station observations (Gandoin and Garza, 2024). This does not affect the proof of concept of the RF methodology, but a more operationally oriented assessment should use ERA5 and station observations as RF training data.

The effects of SSWs have been briefly discussed here but not thoroughly investigated, as the primary focus has been on the impact of stratospheric conditions on seasonal predictability. Our results, however, hint at the importance of dynamics with spatial scales smaller than pan-circumpolar to target the predictability of seasons with more frequent extreme winds, which would require a more spatially detailed description of the dynamics of SSWs.

6 Summary and conclusion

The purpose of this research is to improve the month-to-month storm prediction skill by using different machine learning models. In this work, we develop statistical and machine-learning models to quantify the relationship between large-scale stratospheric conditions in one winter month and observed storminess in the North Sea during the following month.

The study uses techniques such as PCA for dimensionality reduction and Random Forest regression for prediction. The models extract dominant patterns in stratospheric temperature, upper-tropospheric geopotential height, and stratospheric wind anomalies from 1940 to 2024. To test physical attributes, we use the ACE2 climate emulator to conduct controlled experiments in which we perturb the initial stratospheric conditions. By adding observed anomalies, such as cold temperature patterns and wind anomalies from December 2015, into different historical years, we can observe their impact on the subsequent month's surface winds. These experiments allow us to assess whether specific stratospheric states actively contribute to a stormier or calmer North Sea winter, rather than just correlating with it.

Winter storms are among the most damaging climate hazards affecting northwestern Europe, with the North Sea region experiencing particularly high exposure due to frequent extratropical cyclones and strong surface winds (Donat et al., 2011; **?**). Improving understanding of and seasonal prediction of North Sea storminess is highly relevant to coastal safety, offshore energy planning, and climate risk management.

The key findings begin with the ACE2 experiments. By imposing the colder stratospheric temperature anomalies and the associated wind patterns observed in December 2015, the simulations were designed to test whether the known link between lower polar stratosphere dynamics and surface weather can be used for a month-to-month prediction scheme: a perturbed stratosphere can intensify surface winds in the following month. The model results generally support this hypothesis: in several

https://doi.org/10.5194/egusphere-2026-1225
Preprint. Discussion started: 9 March 2026

cases, surface wind speeds begin to increase after day 7 and continue to strengthen through day 60. However, in one case (2001), no increase in surface wind speed is observed during the 7–60-day period, indicating that the stratospheric state does not solely control enhanced surface winds and that other factors also play a role.

The Random Forest model links December stratospheric and upper-tropospheric atmospheric conditions to January storminess in the North Sea. After preprocessing ERA5 datasets (air temperature at 70 hPa, geopotential height at 200 hPa, and zonal wind at 70 hPa) and reducing dimensionality with PCA, the model achieves predictive skill with correlations of 0.55–0.60 and explains roughly one-third of the observed variability. The results show that the first principal component, representing a strong, dynamically coherent Arctic pattern across all three fields, highlights the central role of the polar vortex. PC5, PC3, and PC2, in contrast, display asymmetric spatial patterns indicative of a distorted polar vortex. When extending the analysis to different month pairs (e.g November predictors to predict December storminess), predictability remains moderately high (r = 0.20–0.36) during the core winter months, when the polar vortex is well developed, but drops sharply during autumn and spring, when the vortex is forming or breaking down. This pattern aligns with the known seasonal cycle of the vortex and the period of strongest stratosphere–troposphere coupling.

In conclusion, our findings from ACE2 experiments and RFR models show a moderately robust link between December stratospheric states and January North Sea storminess. Using these methods, we develop a predictive tool that accounts for approximately 30% of storm variability. These insights represent a significant step toward mitigating the socio-economic risks posed by winter wind extremes in northwestern Europe.

Data availability. Copernicus Climate Change Service, Climate Data Store, (2024): ERA5 post-processed daily-statistics on pressure levels from 1940 to present. Copernicus Climate Change Service (C3S) Climate Data Store (CDS), (Hersbach et al., 2020) [Generated using/Contains modified] Copernicus Climate Change Service information. Neither the European Commission nor ECMWF is responsible for any use that may be made of the Copernicus information or data it contains.

Author contributions. All authors contributed to shaping the overall research goal and discussing the results. P.A. carried out the data preprocessing, developed the storm index, and performed the statistical and machine-learning analysis. P.A. also conducted the ACE2 perturbation experiments and produced all visualisations. E.Z. provided data, contributed to the conceptual design and offered methodological guidance. B.H. supervised the research, supported the scientific framing, and contributed to manuscript revision. P.A. wrote the original draft; all authors reviewed and approved the final manuscript.

Competing interests. The contact author has declared that none of the authors has any competing interests.

https://doi.org/10.5194/egusphere-2026-1225
Preprint. Discussion started: 9 March 2026

Acknowledgements. This work has been conducted within the project NECO: "Natural hazards and response of the marine ecosystem - causal relationship and predictability", funded by the Federal Ministry of Research, Technology and Space (BMFTR) under funding code FKZ 03F0950A. We thank the German Computing Center (DKRZ) for providing their computing resources. We also thank the authors of the ACE2 emulator (Watt-Meyer et al., 2025) for making the trained model available to the research community.

https://doi.org/10.5194/egusphere-2026-1225
Preprint. Discussion started: 9 March 2026

References

Ai2: ACE2-ERA5, https://doi.org/10.57967/HF/5377, 2025.

Baldwin, M. P., Ayarzagüena, B., Birner, T., Butchart, N., Butler, A. H., Charlton-Perez, A. J., Domeisen, D. I. V., Garfinkel, C. I., Garny, H., Gerber, E. P., Hegglin, M. I., Langematz, U., and Pedatella, N. M.: Sudden Stratospheric Warmings, Reviews of Geophysics, 59, https://doi.org/10.1029/2020rg000708, 2020.

Bellinghausen, K., Hünicke, B., and Zorita, E.: Coherent Modes of Northern Hemisphere Wind Extremes and Their Links to Global Large-Scale Drivers, EGUsphere, 2026, 1–53, https://doi.org/10.5194/egusphere-2026-523, 2026.

Breiman, L.: Random Forests, Machine Learning, 45, 5–32, https://doi.org/10.1023/a:1010933404324, 2001.

Brönnimann, S.: Impact of El Niño–Southern Oscillation on European climate, Reviews of Geophysics, 45, https://doi.org/10.1029/2006rg000199, 2007.

Charlton-Perez, A., Ferranti, L., and Lee, R.: The influence of the stratospheric state on North Atlantic weather regimes, QJ Roy. Meteor. Soc., 144, 1140–1151, Q. J. R. Meteorol. Soc., 144, 1140–1151, https://doi.org/10.1002/qj.3280, 2018.

Domeisen, D. I.: Estimating the frequency of sudden stratospheric warming events from surface observations of the North Atlantic Oscillation, Journal of Geophysical Research: Atmospheres, 124, 3180–3194, https://doi.org/10.1029/2018JD030077, 2019.

Domeisen, D. I. V. and Butler, A. H.: Stratospheric drivers of extreme events at the Earth's surface, Communications Earth amp; Environment, 1, https://doi.org/10.1038/s43247-020-00060-z, 2020.

Donat, M. G., Pardowitz, T., Leckebusch, G. C., Ulbrich, U., and Burghoff, O.: High-resolution refinement of a storm loss model and estimation of return periods of loss-intensive storms over Germany, Natural Hazards and Earth System Sciences, 11, 2821–2833, https://doi.org/10.5194/nhess-11-2821-2011, 2011.

Feser, F., Barcikowska, M., Krueger, O., Schenk, F., Weisse, R., and Xia, L.: Storminess over the North Atlantic and northwestern Europe—A review, Quarterly Journal of the Royal Meteorological Society, 141, 350–382, https://doi.org/10.1002/qj.2364, 2014.

Gagne II, D. J., Haupt, S. E., Nychka, D. W., and Thompson, G.: Interpretable deep learning for spatial analysis of severe hailstorms, Monthly Weather Review, 147, 2827–2845, https://doi.org/10.1175/MWR-D-18-0316.1, 2019.

Gandoin, R. and Garza, J.: Underestimation of strong wind speeds offshore in ERA5: evidence, discussion and correction, Wind Energy Science, 9, 1727–1745, https://doi.org/10.5194/wes-9-1727-2024, 2024.

Gao, J., Heinselman, P. L., Xue, M., Wicker, L. J., Yussouf, N., Stensrud, D. J., and Droegemeier, K. K.: The Numerical Prediction of Severe Convective Storms: Advances in Research and Applications, Remaining Challenges, and Outlook for the Future, Elsevier, ISBN 9780124095489, https://doi.org/10.1016/b978-0-323-96026-7.00127-2, 2024.

Gershunov, A. and Barnett, T. P.: Interdecadal modulation of ENSO teleconnections, Bulletin of the American Meteorological Society, 79, 2715–2726, https://doi.org/10.1175/1520-0477(1998)079<2715:IMOET>2.0.CO;2, 1998.

Hersbach, H., Bell, B., Berrisford, P., Hirahara, S., Horányi, A., Muñoz-Sabater, J., Nicolas, J., Peubey, C., Radu, R., Schepers, D., Simmons, A., Soci, C., Abdalla, S., Abellan, X., Balsamo, G., Bechtold, P., Biavati, G., Bidlot, J., Bonavita, M., De Chiara, G., Dahlgren, P., Dee, D., Diamantakis, M., Dragani, R., Flemming, J., Forbes, R., Fuentes, M., Geer, A., Haimberger, L., Healy, S., Hogan, R. J., Hólm, E., Janisková, M., Keeley, S., Laloyaux, P., Lopez, P., Lupu, C., Radnoti, G., de Rosnay, P., Rozum, I., Vamborg, F., Villaume, S., and Thépaut, J.: The ERA5 global reanalysis, Quarterly Journal of the Royal Meteorological Society, 146, 1999–2049, https://doi.org/10.1002/qj.3803, 2020.

https://doi.org/10.5194/egusphere-2026-1225
Preprint. Discussion started: 9 March 2026

Hurrell, J. W., Kushnir, Y., Ottersen, G., and Visbeck, M.: An overview of the North Atlantic Oscillation, p. 1–35, American Geophysical Union, ISBN 0875909949, https://doi.org/10.1029/134gm01, 2003.

Kew, S. F., Selten, F. M., Lenderink, G., and Hazeleger, W.: The simultaneous occurrence of surge and discharge extremes for the Rhine delta, Natural Hazards and Earth System Sciences, 13, 2017–2029, https://doi.org/10.5194/nhess-13-2017-2013, 2013.

Kidston, J., Scaife, A. A., Hardiman, S. C., Mitchell, D. M., Butchart, N., Baldwin, M. P., and Gray, L. J.: Stratospheric influence on tropospheric jet streams, storm tracks and surface weather, Nature Geoscience, 8, 433–440, https://doi.org/10.1038/ngeo2424, 2015.

Krieger, D., Brune, S., Baehr, J., and Weisse, R.: Improving seasonal predictions of German Bight storm activity, Natural Hazards and Earth System Sciences, 24, 1539–1554, https://doi.org/10.5194/nhess-24-1539-2024, 2024.

Kushnir, Y.: Interdecadal Variations in North Atlantic Sea Surface Temperature and Associated Atmospheric Conditions, Journal of Climate, 7, 141–157, https://doi.org/10.1175/1520-0442(1994)007<0141:ivinas>2.0.co;2, 1994.

Limpasuvan, V., Hartmann, D. L., Thompson, D. W. J., Jeev, K., and Yung, Y. L.: Stratosphere-troposphere evolution during polar vortex intensification, Journal of Geophysical Research: Atmospheres, 110, https://doi.org/10.1029/2005jd006302, 2005.

McKenna, C. M. and Maycock, A. C.: The Role of the North Atlantic Oscillation for Projections of Winter Mean Precipitation in Europe, Geophysical Research Letters, 49, https://doi.org/10.1029/2022gl099083, 2022.

Mouallem, J., Yao, W., Harris, L., Lin, S., and Chen, X.: A Minimal, Adiabatic Example of Sudden Stratospheric Warming, Journal of Advances in Modeling Earth Systems, 17, https://doi.org/10.1029/2024ms004760, 2025.

Pinto, J. G. and Raible, C. C.: Past and recent changes in the North Atlantic oscillation, WIREs Climate Change, 3, 79–90, https://doi.org/10.1002/wcc.150, 2011.

Pu, Z. and Kalnay, E.: Numerical Weather Prediction Basics: Models, Numerical Methods, and Data Assimilation, p. 1–31, Springer Berlin Heidelberg, ISBN 9783642404573, https://doi.org/10.1007/978-3-642-40457-3_11-1, 2018.

Scaife, A. A., Arribas, A., Blockley, E., Brookshaw, A., Clark, R. T., Dunstone, N., Eade, R., Fereday, D., Folland, C. K., Gordon, M., Hermanson, L., Knight, J. R., Lea, D. J., MacLachlan, C., Maidens, A., Martin, M., Peterson, A. K., Smith, D., Vellinga, M., Wallace, E., Waters, J., and Williams, A.: Skillful long-range prediction of European and North American winters, Geophysical Research Letters, 41, 2514–2519, https://doi.org/10.1002/2014gl059637, 2014.

Schade, N. H.: Evaluating the atmospheric drivers leading to the December 2014 flood in Schleswig-Holstein, Germany, Earth System Dynamics, 8, 405–418, https://doi.org/10.5194/esd-8-405-2017, 2017.

Schade, N. H., Jensen, C., and Kruschke, T.: Large scale atmospheric conditions favoring storm surges in the North and Baltic Seas and possible future changes, Frontiers in Environmental Science, 13, https://doi.org/10.3389/fenvs.2025.1601836, 2025.

Schemm, S., Rüdisühli, S., and Sprenger, M.: The life cycle of upper-level troughs and ridges: a novel detection method, climatologies and Lagrangian characteristics, Weather and Climate Dynamics, 1, 459–479, https://doi.org/10.5194/wcd-1-459-2020, 2020.

Sung, M.-K., Ham, Y.-G., Kug, J.-S., and An, S.-I.: An alterative effect by the tropical North Atlantic SST in intraseasonally varying El Niño teleconnection over the North Atlantic, Tellus A: Dynamic Meteorology and Oceanography, 65, 19 863, https://doi.org/10.3402/tellusa.v65i0.19863, 2013.

Tian, Q., Luo, W., Tian, Y., Gao, H., Guo, L., and Jiang, Y.: Prediction of storm surge in the Pearl River Estuary based on data-driven model, Frontiers in Marine Science, 11, https://doi.org/10.3389/fmars.2024.1390364, 2024.

Urraca, R., Huld, T., Gracia-Amillo, A., Martinez-de Pison, F. J., Kaspar, F., and Sanz-Garcia, A.: Evaluation of global horizontal irradiance estimates from ERA5 and COSMO-REA6 reanalyses using ground and satellite-based data, Solar Energy, 164, 339–354, https://doi.org/10.1016/j.solener.2018.02.059, 2018.

https://doi.org/10.5194/egusphere-2026-1225
Preprint. Discussion started: 9 March 2026

Wang, L., Ting, M., and Kushner, P. J.: A robust empirical seasonal prediction of winter NAO and surface climate, Scientific Reports, 7, https://doi.org/10.1038/s41598-017-00353-y, 2017.

Watt-Meyer, O., Dresdner, G., McGibbon, J., Clark, S. K., Henn, B., Duncan, J., Brenowitz, N. D., Kashinath, K., Pritchard, M. S., Bonev, B., et al.: ACE: A fast, skillful learned global atmospheric model for climate prediction, arXiv preprint arXiv:2310.02074, https://doi.org/10.48550/arXiv.2310.02074, 2023.

Watt-Meyer, O., Henn, B., McGibbon, J., Clark, S. K., Kwa, A., Perkins, W. A., and Bretherton, C.: ACE2: Accurately learning sub-seasonal to decadal atmospheric variability and forced responses. npj Climate and Atmospheric Science, 8 (1), 205, URL https://doi.org/10.1038/s41612-025-01090-0, https://doi.org/10.1038/s41612-025-01090-0, 2025.

Xie, Y., Shang, S., Chen, J., Zhang, F., He, Z., Wei, G., Wu, J., Zhu, B., and Zeng, Y.: Fast Storm Surge Ensemble Prediction using Searching Optimization of a Numerical Scenario Database, Weather and Forecasting, https://doi.org/10.1175/waf-d-20-0205.1, 2021.

Zhang, C., Zhang, J., Xia, X., Song, J., Li, D., and Tian, W.: Impacts of stratospheric polar vortex changes on tropospheric blockings over the Atlantic region, Climate Dynamics, 62, 4829–4848, https://doi.org/10.1007/s00382-023-07092-z, 2024.